A Theoretical Results and Proofs

Theorem 1. *Given a 3D linear tensor field $T(x,y,z) = T_0 + xT_x + yT_y + zT_z$, a mode value $0 < \mu < 1$, and a unit vector v_2, the number of points on the generalized mode μ surface with $\pm v_2$ as its medium eigenvector is the same as the number of real eigenvalues of the 2D asymmetric tensor $A = R_{\frac{\theta}{2}+\frac{\pi}{4}} \overline{T}' R_{\frac{\theta}{2}-\frac{\pi}{4}}$ where $\overline{T}'$ is the projection of characteristic tensor $\overline{T}$ onto the plane P with normal v_2, $\theta = \arcsin(\sqrt{3}\tan(\frac{1}{3}\arcsin(\mu)))$, and $R_\phi = \begin{pmatrix} \cos\phi & -\sin\phi \\ \sin\phi & \cos\phi \end{pmatrix}$. The real-valued eigenvectors of A give rise to the dominant eigenvectors of the corresponding points in the generalized mode μ surface.*

Proof. As pointed out in [32], given a tensor $t = \lambda_1 v_1 v_1^T + \lambda_2 v_2 v_2^T + \lambda_3 v_3 v_3^T$ in the linear tensor field $T(x,y,z) = T_0 + xT_x + yT_y + zT_z$, where v_1, v_2, and v_3 are respectively the major, medium, and minor eigenvectors, we have

$$v_1^T \overline{T} v_1 + v_2^T \overline{T} v_2 + v_3^T \overline{T} v_3 = 0. \tag{15}$$

In addition, since $\overline{T}$ is the characteristic tensor of $T(x,y,z)$,

$$\begin{aligned} 0 &= \left\langle \overline{T}, \lambda_1 v_1 v_1^T + \lambda_2 v_2 v_2^T + \lambda_3 v_3 v_3^T \right\rangle \\ &= \lambda_1 \operatorname{trace}(\overline{T} v_1 v_1^T) + \lambda_2 \operatorname{trace}(\overline{T} v_2 v_2^T) + \lambda_3 \operatorname{trace}(\overline{T} v_3 v_3^T) \\ &= \lambda_1 v_1^T \overline{T} v_1 + \lambda_2 v_2^T \overline{T} v_2 + \lambda_3 v_3^T \overline{T} v_3. \end{aligned} \tag{16}$$

according to the *cyclic property of trace* [12].

Combining this equation with Equation 15, we have

$$0 = (\lambda_1 - \lambda_2) v_1^T \overline{T} v_1 - (\lambda_2 - \lambda_3) v_3^T \overline{T} v_3. \tag{17}$$

Notice that the major eigenvector v_1 and minor eigenvector v_3 must be inside P, the plane that contains the point where t occurs in the field and whose normal is v_2. Let v_1' and v_3' be v_1 and v_3 expressed in the coordinate system of P. Consequently, Equation 17 can be rewritten as the following:

$$0 = (\lambda_1 - \lambda_2) v_1'^T \overline{T}' v_1' - (\lambda_2 - \lambda_3) v_3'^T \overline{T}' v_3'. \tag{18}$$

We first consider the case when $\mu(t) > 0$ and use the right-handed coordinate system where v_3 is the horizontal axis and v_1 is the vertical axis.

For simplification purposes, we define $u = kv_1' + lv_3'$ and $w = kv_1' - lv_3'$ where $k = \sqrt{\frac{\lambda_1 - \lambda_2}{\lambda_1 - \lambda_3}}$ and $l = \sqrt{\frac{\lambda_2 - \lambda_3}{\lambda_1 - \lambda_3}}$. Therefore, $v_1' = \frac{u+w}{2k}$ and $v_3' = \frac{u-w}{2l}$.

It is straightforward to verify that u and w both have unit length. Moreover, since both v_1' and v_3' are unit vectors and have the same length, it can be verified that

$$u \cdot w = k^2 - l^2 = \frac{\lambda_1 + \lambda_3 - 2\lambda_2}{\lambda_1 - \lambda_3}. \tag{19}$$

Since $\lambda_1 + \lambda_2 + \lambda_3 = 0$, we have

$$\lambda_1 + \lambda_3 - 2\lambda_2 = -3\lambda_2 = \sqrt{6}\sin(\frac{1}{3}\arcsin(\mu)). \tag{20}$$

Similarly, it can be shown that

$$\lambda_1 - \lambda_3 = \sqrt{2 - 3\lambda_2^2} = \sqrt{2}\cos(\frac{1}{3}\arcsin(\mu)). \tag{21}$$

Consequently,

$$u \cdot w = \frac{\lambda_1 + \lambda_3 - 2\lambda_2}{\lambda_1 - \lambda_3} = \sqrt{3}\tan(\frac{1}{3}\arcsin(\mu)) = \sin\theta. \tag{22}$$

Notice that since $k \geq 0$ and $l \geq 0$, w is always counterclockwise of u. Therefore, w is obtained by rotating u counterclockwise by $\frac{\pi}{2} - \theta$. Note that Equation 18 can be rewritten in terms of u and w as $w^T \overline{T}' u = 0$, or equivalently $w \cdot (\overline{T}' u) = 0$. That is, $w \perp \overline{T}' u$.

As v_1' is a bisector of u and w, v_1' can be obtained by either rotating u counterclockwise by $\frac{\pi}{4} - \frac{\theta}{2}$ or rotating w counterclockwise by $\frac{\theta}{2} - \frac{\pi}{4}$. That is, $u = R_{\frac{\theta}{2}-\frac{\pi}{4}} v_1'$ and $w = R_{\frac{\pi}{4}-\frac{\theta}{2}} v_1'$. Therefore,

$$R_{\frac{\pi}{4}-\frac{\theta}{2}} v_1' \perp \overline{T}' R_{\frac{\theta}{2}-\frac{\pi}{4}} v_1'. \tag{23}$$

Since $v_3' \perp v_1'$, we have $v_1' = R_{-\frac{\pi}{2}} v_3'$. Consequently, $R_{\frac{\pi}{4}-\frac{\theta}{2}} R_{-\frac{\pi}{2}} v_3' \perp \overline{T}' R_{\frac{\theta}{2}-\frac{\pi}{4}} v_1'$, which is equivalent to $R_{-\frac{\pi}{4}-\frac{\theta}{2}} v_3' \perp \overline{T}' R_{\frac{\theta}{2}-\frac{\pi}{4}} v_1'$. Rotating both sides conterclockwise by $\frac{\pi}{4} + \frac{\theta}{2}$, we have

$$v_3' \perp R_{\frac{\pi}{4}+\frac{\theta}{2}} \overline{T}' R_{\frac{\theta}{2}-\frac{\pi}{4}} v_1'. \tag{24}$$

Recall that $A = R_{\frac{\theta}{2}+\frac{\pi}{4}} \overline{T}' R_{\frac{\theta}{2}-\frac{\pi}{4}}$. Then $v_3' \perp A v_1'$.

This means that Av_1' must be orthogonal to a vector that is orthogonal to v_1'. As v_1' is in two dimensions, this implies that Av_1' is a scalar multiple of v_1'. Consequently, v_1' is an eigenvector of A.

In the case where $\mu(t) < 0$, we use the right-handed coordinate system of P such that v_1 is now the horizontal axis and v_3 is the vertical axis.

We again define $u = kv_1' + lv_3'$ but negate w, i.e. $w = -kv_1' + lv_3'$. We can still show that u and w are unit vectors and $u \cdot w = \sqrt{3}\tan(\frac{1}{3}\arcsin(\mu))$.

From here, we follow the same argument for the case where $\mu(t) > 0$ except that we need to reverse the roles of v_1' and v_3'. This leads to that v_3' is an eigenvector of $A = R_{\frac{\theta}{2}+\frac{\pi}{4}} \overline{T}' R_{\frac{\theta}{2}-\frac{\pi}{4}}$.

We now consider a number of cases. First, when A has zero real eigenvalues, its eigenvectors must be complex-valued. Since the eigenvectors of a 3D symmetric tensor cannot be complex-valued, there are no points on the generalized mode μ surface with v_2 as its medium eigenvectors.

When A has only one real eigenvalue, there is only one point in the generalized mode μ surface whose medium eigenvector is v_2. Depending on the sign of the mode value of this point, either its major eigenvector v_1 ($\mu(t) > 0$) or minor eigenvector v_3 ($\mu(t) < 0$) is given by the corresponding eigenvector of A. Recall that the dominant eigenvector is the major eigenvector v_1 when $\mu(t) = \mu > 0$ and the minor eigenvector v_3 when $\mu(t) = -\mu < 0$. Therefore, the eigenvector of A gives the dominant eigenvector of the point in the generalized mode μ surface.

To see the uniqueness, we note that if there is another point in the generalized mode μ surface with the same combination of v_1, v_2, v_3 and $\mu(t)$, then the tensor must be a multiple of t. However, as pointed out by Roy et al. [32], if a tensor t appears in a 3D linear tensor field, then none of its multiples can appear in the same field. Consequently, there is only one point in the generalized mode μ surface with v_2 as its medium eigenvector.

On the other hand, when A has two real eigenvalues, the major eigenvector and the minor eigenvector of A *each* corresponds to a point in the generalized mode μ surface whose medium eigenvectors are given by v_2. If the point has a positive mode value, its major eigenvector v_1 is given by the corresponding eigenvector of A. In contrast, if the point has a negative mode value, its minor eigenvector v_3 is given by the corresponding eigenvector of A.

What remains to be shown is that using $-v_2$ as the medium eigenvector, we arrive at the same set of points as using v_2. Again, we have the two cases $\mu(t) > 0$ and $\mu(t) < 0$.

For the first case, note that the rotations in the definition of A are around v_2, and they are reversed when $-v_2$ is chosen as the medium eigenvector. Assume that A's eigenvalues are $\hat{\lambda}_1$ and $\hat{\lambda}_2$, and that v_1' is the eigenvector corresponding to $\hat{\lambda}_1$. Then we find the eigenvalue on the opposite side of the sphere with

$$\begin{aligned} R_{-(\frac{\theta}{2}+\frac{\pi}{4})}\overline{T}'R_{-(\frac{\theta}{2}-\frac{\pi}{4})}v_1' &= A^T v_1' \\ &= R_{\frac{\pi}{2}}(R_{-\frac{\pi}{2}}A^T R_{\frac{\pi}{2}})R_{-\frac{\pi}{2}}v_1' \\ &= R_{\frac{\pi}{2}}adj(A)R_{-\frac{\pi}{2}}v_1' \\ &= R_{\frac{\pi}{2}}adj(A)v_3' \\ &= R_{\frac{\pi}{2}}\hat{\lambda}_2 v_3' \\ &= \hat{\lambda}_2 R_{\frac{\pi}{2}}v_3' \\ &= \hat{\lambda}_2 v_1' \end{aligned} \tag{25}$$

where we have used a property of asymmetric 2x2 tensors [33] that if $A = \begin{bmatrix} a & b \\ c & d \end{bmatrix}$ is a 2D asymmetric tensor and R_θ is the two-dimensional counterclockwise rotation matrix of angle θ,

$$R_{-\frac{\pi}{2}}A^T R_{\frac{\pi}{2}} = \begin{bmatrix} d & -b \\ -c & a \end{bmatrix} = \text{adj}(A) \tag{26}$$

is the adjugate of A, whose eigenvectors are the same as A's and the roles of whose major and minor eigenvalues are swapped. Consequently, the point on the generalized mode μ surface with v_1 given by the major eigenvector of $A(v_2)$ is the same point whose v_1 is given by the minor eigenvector of $A(-v_2)$.

A similar argument applies when $\mu(t) < 0$.

To summarize, v_2 and $-v_2$ correspond to the same set of points in the generalized mode μ surface. Moreover, when there are two points with v_2 and $-v_2$ as medium eigenvectors, each of $A(v_2)$ and $A(-v_2)$ corresponds to exactly *one* point in the generalized mode μ surface whose dominant eigenvector (as a 3D symmetric tensor) is given by the major eigenvector of A (as an asymmetric tensor). □

Theorem 2. *Given a 3D linear tensor field $T(x,y,z) = T_0 + xT_x + yT_y + zT_z$ and a mode value μ, the real domain in the medium eigenvector manifold corresponding to μ is characterized by $\frac{1}{2} - v_2^T\overline{T}'^2 v_2 + \frac{1}{4}\cos^2\theta(v_2^T\overline{T}'v_2)^2 \geq 0$ where $\theta = \arcsin(\sqrt{3}\tan(\frac{1}{3}\arcsin(\mu)))$. The boundary between the real and complex domain occurs if and only if the equal sign holds.*

Proof. Let $\overline{T'}$ be the projection of the characteristic tensor $\overline{T}$ of the tensor field onto the plane perpendicular to unit medium eigenvectors v_2. We consider the asymmetric tensor field $A(v_2) = R_{\frac{\theta}{2}+\frac{\pi}{4}}\overline{T}'(v_2)R_{\frac{\theta}{2}-\frac{\pi}{4}}$.

As mentioned in [36], a 2×2 asymmetric matrix A can be uniquely decomposed as follows:

$$A = \gamma_d \begin{bmatrix} 1 & 0 \\ 0 & 1 \end{bmatrix} + \gamma_r \begin{bmatrix} 0 & -1 \\ 1 & 0 \end{bmatrix} + \gamma_s \begin{bmatrix} \cos\tau & \sin\tau \\ \sin\tau & -\cos\tau \end{bmatrix} \tag{27}$$

where γ_d, γ_r, and γ_r are the isotropic, rotational, and anisotropic components, respectively. Note that τ gives rise to the eigenvector information of A. Depending on the discriminant of $\Delta = \gamma_s^2 - \gamma_r^2$, A has either two real eigenvalues ($\Delta > 0$) or two complex-valued eigenvalues ($\Delta < 0$). When $\Delta = 0$, A has a pair of repeating eigenvalues. For our asymmetric tensor field, this implies that v_2 is on the complex domain boundary in the medium eigenvector manifold. Notice that this condition is both necessary and sufficient. To compute Δ, we need to compute both γ_d and γ_r.

$$\begin{aligned} \gamma_d &= \frac{1}{2}\text{trace}(A) \\ &= \frac{1}{2}\text{trace}(R_{\frac{\theta}{2}+\frac{\pi}{4}}\overline{T}'R_{\frac{\theta}{2}-\frac{\pi}{4}}) \\ &= \frac{1}{2}\text{trace}(R_{\frac{\theta}{2}-\frac{\pi}{4}}R_{\frac{\theta}{2}+\frac{\pi}{4}}\overline{T}') \\ &= \frac{1}{2}\text{trace}(R_\theta\overline{T}') \\ &= \frac{1}{2}\text{trace}(\cos\theta\,\mathbb{I}\,\overline{T}') + \frac{1}{2}\text{trace}\left(\sin\theta\begin{bmatrix} 0 & -1 \\ 1 & 0 \end{bmatrix}\overline{T}'\right) \\ &= \cos\theta\frac{\text{trace}(\overline{T}')}{2} \end{aligned} \tag{28}$$

where the second term vanishes because $\overline{T'}$ is symmetric.

Since trace is the same in any basis, we have

$$\text{trace}(\overline{T}') = v_1'^T\overline{T}'v_1' + v_3'^T\overline{T}'v_3'.$$

Recall that $\overline{T}'$, v_1', and v_3' are respectively the projection of $\overline{T}$, v_1, and v_3 onto the plane perpendicular to v_2. Thus,

$$v_1'^T\overline{T}'v_1' + v_3'^T\overline{T}'v_3' = v_1^T\overline{T}v_1 + v_3^T\overline{T}v_3 = -v_2^T\overline{T}v_2 \tag{29}$$

in which the second equality above comes from rearranging Equation 15.

Consequently,

$$\gamma_d = -\cos\theta\frac{v_2^T\overline{T}v_2}{2}. \tag{30}$$

A similar calculation shows that

$$\gamma_r = \sin\theta\frac{\text{trace}(\overline{T}')}{2} = -\sin\theta\frac{v_2^T\overline{T}v_2}{2}. \tag{31}$$

Notice that $\gamma_d^2 + \gamma_r^2 = (\frac{v_2^T\overline{T}v_2}{2})^2$. To compute γ_s it is convenient to find the squared magnitude of A, which is

$$\text{trace}(A^TA) = \text{trace}((R_{\frac{\theta}{2}+\frac{\pi}{4}}\overline{T}'R_{\frac{\theta}{2}-\frac{\pi}{4}})^TR_{\frac{\theta}{2}+\frac{\pi}{4}}\overline{T}'R_{\frac{\theta}{2}-\frac{\pi}{4}}) = \text{trace}(\overline{T}'^2). \tag{32}$$

Since v_2 has unit length, the matrix $\mathbb{I}-v_2v_2^T$ is a projection matrix and is thus equal to its square. Using this to project the tensor $\overline{T}$, we have

$$\begin{aligned}\text{trace}(\overline{T}'^2) &= \text{trace}((\mathbb{I}-v_2v_2^T)\overline{T}(\mathbb{I}-v_2v_2^T)^2\overline{T}(\mathbb{I}-v_2v_2^T))\\ &= \text{trace}(\overline{T}(\mathbb{I}-v_2v_2^T)^2\overline{T}(\mathbb{I}-v_2v_2^T)^2)\\ &= \text{trace}(\overline{T}(\mathbb{I}-v_2v_2^T)\overline{T}(\mathbb{I}-v_2v_2^T))\\ &= \text{trace}(\overline{T}^2) - \text{trace}(\overline{T}v_2v_2^T\overline{T})\\ &- \text{trace}(\overline{T}^2v_2v_2^T) + \text{trace}(\overline{T}v_2v_2^T\overline{T}v_2v_2^T)\\ &= 1-2v_2^T\overline{T}^2v_2+(v_2^T\overline{T}v_2)^2. \end{aligned}\tag{33}$$

Because A's magnitude is $2(\gamma_r^2+\gamma_s^2+\gamma_d^2)$, we can use this to find γ_s.

$$\begin{aligned}\gamma_s^2 &= \frac{1}{2}\text{trace}(A^TA) - \gamma_d^2 - \gamma_r^2\\ &= \frac{1}{2} - v_2^T\overline{T}^2v_2 + \frac{1}{2}(v_2^T\overline{T}v_2)^2 - \left(\frac{v_2^T\overline{T}v_2}{2}\right)^2\\ &= \frac{1}{2} - v_2^T\overline{T}^2v_2 + \frac{1}{4}(v_2^T\overline{T}v_2)^2. \end{aligned}\tag{34}$$

The real domain is characterized by $\gamma_s^2 \geq \gamma_r^2$, i.e.

$$\frac{1}{2} - v_2^T\overline{T}^2v_2 + \frac{1}{4}(v_2^T\overline{T}v_2)^2 \geq (-\sin\theta\frac{v_2^T\overline{T}v_2}{2})^2 \tag{35}$$

or equivalently, $\frac{1}{2} - v_2^T\overline{T}^2v_2 + \frac{1}{4}\cos^2\theta(v_2^T\overline{T}v_2)^2 \geq 0$. The complex domain boundary is thus

$$\frac{1}{2} - v_2^T\overline{T}^2v_2 + \frac{1}{4}\cos^2\theta(v_2^T\overline{T}v_2)^2 = 0 \tag{36}$$

□

Corollary 3. *Given a 3D linear tensor field $T(x,y,z) = T_0 + xT_x + yT_y + zT_z$ and two mode values μ_1 and μ_2 such that $0 \leq \mu_1 < \mu_2 \leq 1$, the complex domain on the medium eigenvector manifold corresponding to μ_1 is a proper subset of that corresponding to μ_2.*

Proof. The complex domain is characterized by the following inequality opposite that for the real domain, i.e.,

$$\frac{1}{2} - v_2^T\overline{T}^2v_2 + \frac{1}{4}\cos^2\theta(v_2^T\overline{T}v_2)^2 < 0. \tag{37}$$

Recall that $\theta = \arcsin(\sqrt{3}\tan(\frac{1}{3}\arcsin(\mu)))$ (Theorem 1), which implies θ is monotonically increasing with respect to mode values μ. Consider the range of θ which is $[0,\frac{\pi}{2}]$, $\cos^2\theta$ is a monotonically decreasing function with respect to μ. That is, for $\mu_1 < \mu_2$, their corresponding θ's satisfy $cos^2\theta_1 > \cos^2\theta_2$.

Consequently, a unit vector v_2 that satisfies

$$\frac{1}{2} - v_2^T\overline{T}^2v_2 + \frac{1}{4}\cos^2\theta_1(v_2^T\overline{T}v_2)^2 < 0 \tag{38}$$

must also satisfy

$$\frac{1}{2} - v_2^T\overline{T}^2v_2 + \frac{1}{4}\cos^2\theta_2(v_2^T\overline{T}v_2)^2 < 0. \tag{39}$$

That is, if v_2 is in the complex domain for μ_1 then it must also reside in the complex domain μ_2. The reverse is not true. Consequently, the complex domain for μ_1 is a proper subset of that of μ_2.

□

Lemma 4. *Given a 3D linear tensor field $T(x,y,z) = T_0 + xT_x + yT_y + zT_z$ and a mode value μ, the complex domain boundary corresponding to μ is parameterizable by $\alpha = v_2\overline{T}v_2$.*

Proof. Let $\overline{\lambda}_1 \geq \overline{\lambda}_2 \geq \overline{\lambda}_3$ be the eigenvalues of $\overline{T}$ and $\bar{v}_1$, $\bar{v}_2$, and $\bar{v}_3$ be the corresponding eigenvectors. For convenience, we choose the coordinate system $\{\bar{v}_1,\bar{v}_2,\bar{v}_3\}$ in which $\overline{T}$ is a diagonal matrix. Let $v_2 = \begin{bmatrix}a\\b\\c\end{bmatrix}$ and $m = \begin{bmatrix}m_x\\m_y\\m_z\end{bmatrix} = \begin{bmatrix}a^2\\b^2\\c^2\end{bmatrix}$. Equation 36 implies

$$\begin{aligned}0 &= 1-2(m_x\overline{\lambda}_1^2 + m_y\overline{\lambda}_2^2 + m_z\overline{\lambda}_3^2)\\ &+ \frac{1}{2}\cos^2\theta(m_x\overline{\lambda}_1 + m_y\overline{\lambda}_2 + m_z\overline{\lambda}_3)^2. \end{aligned}\tag{40}$$

This equation's dependence on only $m_x = a^2$, $m_y = b^2$, and $m_z = c^2$ implies an eight-fold symmetry for the medium eigenvector manifold, and thus the complex domain boundary. That is, if a unit vector (a,b,c) is on the complex domain boundary, so is $(\pm a,\pm b,\pm c)$.

Therefore, we only need to parameterize the segment of the complex domain boundary where $a,b,c \geq 0$. The other seven segments can be parameterized in a similar fashion.

Notice that m is always on the plane $m_x+m_y+m_z = \|v_2\|^2 = 1$. In the coordinate system

$$\alpha = \overline{\lambda}_1m_x + \overline{\lambda}_2m_y + \overline{\lambda}_3m_z = v_2^T\overline{T}v_2 \tag{41}$$

$$\beta = \overline{\lambda}_1^2m_x + \overline{\lambda}_2^2m_y + \overline{\lambda}_3^2m_z = v_2^T\overline{T}^2v_2 \tag{42}$$

Equation 40 becomes

$$0 = 1-2\beta+\frac{1}{2}\cos^2\theta\alpha^2 \tag{43}$$

which is the equation of a parabola that can be parameterized by α. Each α gives one corresponding β from Equation 43 and thus one point on the segment of the complex domain boundary where $a,b,c \geq 0$. □

Theorem 5. *Given a 3D linear tensor field $T(x,y,z) = T_0 + xT_x + yT_y + zT_z$, let $\overline{\mu}$ is the mode of the characteristic tensor $\overline{T}$ and $\mu_0 = \sqrt{1-\overline{\mu}^2}$. The topology of the generalized mode μ surface is a topological torus when $\mu > \mu_0$ and a topological double-torus when $\mu < \mu_0$.*

Proof. We reuse the expressions m_x, m_y, m_z, α, and β from Lemma 4. Note that $m_x \geq 0$, $m_y \geq 0$, $m_z \geq 0$, and $m_x+m_y+m_z = 1$. Therefore, points satisfying these conditions form an equilateral triangle in the plane $m_x+m_y+m_z = 1$, which is illustrated in Figure 11.

Recall that $\overline{T}$ is a unit, traceless tensor with a non-positive determinant (Equation 3). We have

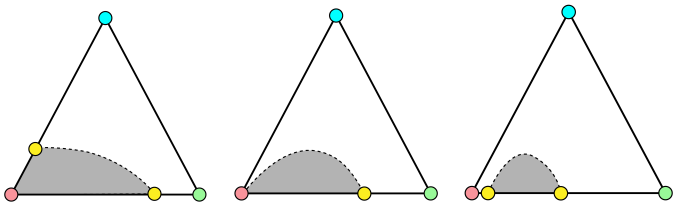

(a) Before bifurcation (b) Bifurcation (c) After bifurcation

Fig. 11: In the triangle bounded by $m_x = 0$, $m_y = 0$, and $m_z = 0$ in the plane $m_x + m_y + m_z = 1$, the corners of the triangle are as follows: $(0,0,1)$ (red), $(1,0,0)$ (green), and $(0,1,0)$ (cyan). When μ decreases, the complex domain (grey regions) reduce in sizes. The complex domain boundary initially intersects each of the $m_x = 0$ and $m_y = 0$ edges once (a). After the bifurcation point (b), the complex domain only intersects the $m_y = 0$ edge (two points). The topology of the generalized mode μ surface depends on whether there is a solution when $m_x = 0$.

$$\overline{\lambda}_1 + \overline{\lambda}_2 + \overline{\lambda}_3 = 0 \tag{44}$$

$$\overline{\lambda}_1^2 + \overline{\lambda}_2^2 + \overline{\lambda}_3^2 = 1 \tag{45}$$

$$\overline{\lambda}_1 \geq \overline{\lambda}_2 \geq 0 \geq \overline{\lambda}_3 \tag{46}$$

Plugging in $\overline{\lambda}_3 = -\overline{\lambda}_1 - \overline{\lambda}_2$ into Equation 45, we have $\overline{\lambda}_1^2 + \overline{\lambda}_1\overline{\lambda}_2 + \overline{\lambda}_2^2 = \frac{1}{2}$. This implies that $\overline{\lambda}_1^2 + \overline{\lambda}_2^2 < \frac{1}{2}$. Consequently, $\overline{\lambda}_1^2 < \frac{1}{2}$, $\overline{\lambda}_2^2 < \frac{1}{2}$, and $\overline{\lambda}_3^2 > \frac{1}{2}$.

For degenerate curves, i.e. $\mu = 1$, $\cos\theta = 0$ and Equation 43 reduces to

$$0 = 1 - 2\beta, \tag{47}$$

which further reduces to $1 - 2\overline{\lambda}_i^2$ at the corners of the triangle. Consequently, this function is negative at $(0,0,1)$ (complex domain) and positive at $(1,0,0)$ and $(0,1,0)$ (real domain). Because the function is linear, its zeroth levelset (complex domain boundary) must intersect each of the edges $m_x = 0$ and $m_y = 0$ exactly once. The subtriangle formed by the two intersection points and $(0,0,1)$ is the complex domain corresponding to $\mu = 1$.

As μ decreases, the complex domain (grey regions in Figure 11) reduce in size (Lemma 4), and the parabola characterized by Equation 43 moves lower while still intersecting $m_x = 0$ and $m_y = 0$ at one point each (the yellow dots on the two edges in (a)). Due to the aforementioned eight-fold symmetry in the medium eigenvector manifold (Lemma 4), this segment of the parabola corresponds to eight segments that constitute the complex domain boundary in the medium eigenvector manifold. Due to the antipodal symmetry, we only consider the four segments where $c > 0$. Since the original parabolic segment touches both the $m_x = 0$ and $m_y = 0$ edges, these four segments will be connected, forming a single loop (Figure 6: the outermost loop). Note that due to the antipodal symmetry, the other four segments in the medium eigenvector manifold ($c < 0$) also form a single loop. Moreover, this loop is to be identified with the loop where $c > 0$. The real domain in the medium eigenvector manifold is thus the part of the sphere between these two loops. Gluing the two loops based on the antipodal symmetry results in a space without a boundary, the torus, which is homeomorphic to the generalized mode μ surface.

The above situation changes when the parabola intersects the corner of $m_x = 0$ and $m_y = 0$ plus an additional point on $m_y = 0$ (Figure 11 (b)). It can be shown that this occurs when $\mu = \sqrt{1 - \overline{\mu}^2}$, which is the bifurcation point. When this happens, the four segments where $c > 0$ form a figure-eight (Figure 6: the loop between the outermost and innermost loops). The real domain in the medium eigenvector manifold is thus the part of the sphere between this loop and its antipodal image. Gluing the two figure-eights results in a surface that has a non-manifold point corresponding to the center of the figure-eight. That is, the generalized mode μ surface in this case is a non-manifold surface.

Decreasing μ further, the parabolic segment only intersects the $m_y = 0$ at two points (Figure 11 (c)). This implies that the four corresponding segments ($c > 0$) in the medium eigenvector manifold form two loops (Figure 6: the innermost loop). Similarly, the four segments ($c < 0$) also form two loops. The real domain is the part of the sphere between the four loops. Gluing the four loops pairwise according to the antipodal symmetry results in a sphere with two handles attached, i.e. double-torus. This is the topology of generalized mode μ surface when $\mu < \mu_0$.

When $\mu = 0$, it is straightforward to verify that the parabolic segment degenerates to a single point, and the aforementioned four loops shrink to two pairs of antipodal points:

$$\left(\pm\sqrt{\frac{\overline{\lambda}_1 - \overline{\lambda}_2}{\overline{\lambda}_1 - \overline{\lambda}_3}} \quad 0 \quad \pm\sqrt{\frac{\overline{\lambda}_2 - \overline{\lambda}_3}{\overline{\lambda}_1 - \overline{\lambda}_3}}\right) \tag{48}$$

Each of the pairs corresponds to one of the two singularities in the medium eigenvector manifold for neutral surfaces [32]. □

Theorem 6. *Given a 3D linear tensor field $T(x,y,z) = T_0 + xT_x + yT_y + zT_z$ and a plane P, the critical points of the mode function on the plane P consist of at most four extrema.*

Proof. On the plane P, the tensor field $T(x,y,z)$ is still a linear tensor field. Therefore, without the loss of generality, we assume the plane P to be the XY plane. If this is not the case, we can simply perform a space transformation so that P becomes the XY plane under the new coordinate system.

In the XY plane, the tensor field has the form $T(x,y) = T_0 + xT_x + yT_y$. We define a map $\chi(x,y) = \frac{T(x,y)}{\|T(x,y)\|}$ from the plane P to the set of unit tensors. Since the tensors on the plane is a combination of T_0, T_x, and T_y, the image of this map together with its negation forms a two-dimensional sphere in the linear subspace spanned by T_0, T_x, and T_y. The map χ is injective because if a tensor has already appeared in a plane, its multiples cannot. Furthermore, χ is locally surjective. Therefore, the set of critical points of the mode function in the plane P has a one-to-one correspondence to the critical points of the mode function on the aforementioned two-dimensional sphere.

The mode of a unit tensor T is $3\sqrt{6}\det(T)$, which means that the critical points of the mode function on the sphere can be found by computing the critical points of the determinant function $\det(T)$ on the sphere. For convenience, we choose T_1, T_2, T_3 to be a orthonormal basis for the space spanned by T_0, T_x, and T_y.

The critical points of a function defined on the sphere are the points where its gradient is colinear to the sphere's normal. Thus, the critical points of the determinant function satisfy

$$\nabla \det(uT_1 + vT_2 + wT_3) \times \begin{bmatrix} u \\ v \\ w \end{bmatrix} = 0 \tag{49}$$

$$u^2 + v^2 + w^2 = 1. \tag{50}$$

Let

$$\nabla \det(uT_1 + vT_2 + wT_3) = \begin{pmatrix} f(u,v,w) \\ g(u,v,w) \\ h(u,v,w) \end{pmatrix} \tag{51}$$

where $f(u,v,w)$, $g(u,v,w)$, and $h(u,v,w)$ are quadratic polynomials. Thus, Equation 49 consists of the following three cubic equations:

$$\begin{aligned} vh(u,v,w) &= wg(u,v,w) \\ wf(u,v,w) &= uh(u,v,w) \\ ug(u,v,w) &= vf(u,v,w). \end{aligned} \tag{52}$$

Together with the condition $u^2 + v^2 + w^2 = 1$, we have an over-determined system of three cubic equations and one quadratic equation. Fortunately, the three cubic equations (Equation 52) are almost redundant. To see this, notice that multiplying the first two of these equations gives rises to

$$vwf(u,v,w)h(u,v,w) = uwg(u,v,w)h(u,v,w) \tag{53}$$

When $w \neq 0$ and $h(u,v,w) \neq 0$, the above equation reduces to the third cubic equation $ug(u,v,w) = vf(u,v,w)$. This shows the redundancy of over-determined system.

After removing the redundant third equation, we get the system

$$vh(u,v,w) = wg(u,v,w) \tag{54}$$

$$wf(u,v,w) = uh(u,v,w) \tag{55}$$

$$u^2 + v^2 + w^2 = 1, \tag{56}$$

which has up to 18 complex solutions based on Bézout's theorem [10]. However, there are some spurious solutions. Note that for $vwf(u,v,w)h(u,v,w) = uwg(u,v,w)h(u,v,w)$ to be equivalent to $ug(u,v,w) = vf(u,v,w)$, we require that $w \neq 0$ and $h(u,v,w) \neq 0$. Assuming that $w = 0$, then we must have $vh(u,v,w) = 0 = uh(u,v,w)$. Since u and v cannot be both zeros (or the vector (u,v,w) is the zero vector), we must have $h(u,v,w) = 0$.

Solutions satisfying $h(u,v,0) = 0$ and $u^2 + v^2 = 1$ have four complex solutions, which are the spurious solutions to our system. Consequently, we have up to $18 - 4 = 14$ complex solutions, thus 14 real solutions at most. Note that if (u,v,w) is a solution, so is $(-u,-v,-w)$. Moreover, they represent the same tensor. Consequently, there are only up to seven real solutions, i.e. up to seven critical points in the mode function in the plane.

The Euler Characteristic of a sphere is two [2], which means that the number of extrema is always two more than the number of saddles according to Morse theory [22]. Together with the fact that there are at most 14 critical points, we can conclude that there are at most eight extrema on the sphere. Since the antipodal points on the sphere give the same point on the plane, we have at most four extrema of the mode function on the plane P.

□

B One More Application Scenario

We provide one more scenario of compression on a block (Figure 12) in which the compressive load is misaligned with the natural geometric orientation of the block due to the addition of a slanted slab on the top of the block. This slanted slab presses down on the block. At the bottom of the block, we also add a full-length layer with a more rigid material. This set-up aims to provide a simplified representation of a tire tread block anchored on some steel belts that hold the tire together while driving on hard pavement. Nonetheless, this type of boundary condition is not limited to tire design. It can be due to misuse of the structure. In particular, both cases exist on tires, i.e. some designs angle tread blocks from the circumferential direction of the tire to facilitate rainwater drainage while irregular wear such as tire cupping induces uneven tread block wear on the shoulders of the tire.

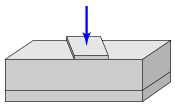

(a)

Fig. 12: Another scenario of compression in a solid block.

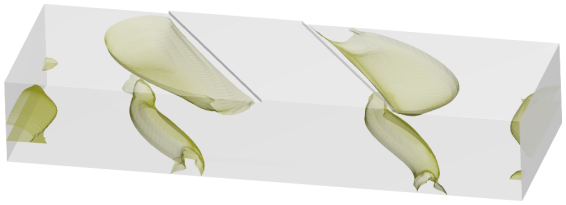

(a) Neutral Surface

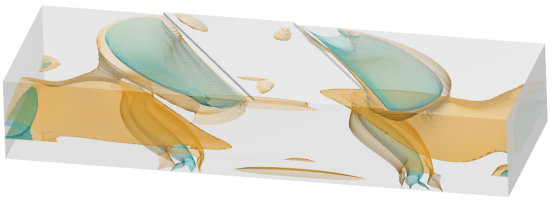

(b) $\mu = \pm 0.4$

Fig. 13: Mode surfaces of stress tensor fields of a rectangular block being pushed down by a slanted slab.

The neutral surface of the stress is shown in Figure 13 (a), which, interestingly, reflects the existence of the slab. In addition, there are two sheets of neutral surfaces attached to the top face, two sheets attached to the sidewalls, and two tubes that connect the front and back faces. The location of these surfaces which indicate pure shear regions match our expectation due to our design of the boundary conditions. In addition, other mode surfaces can also provide meaningful insight. For example, we show the generalized mode 0.4 surface in Figure 13 (b). While the positive part of this surface (teal) and the negative part of the surface (gold) both approximate the neutral surface (Figure 13 (a)), the similarity stops there. The positive part of the mode surface contains additional sheets that are not present in the negative part of the mode surface. This indicates that despite the compression-dominant boundary condition, extension can exist in the middle of the volume. Seeing this positive mode surface confirms the bulging effect from compression.

This visualization can potentially augment the definition of uniaxial compression, the most fundamental description of compression numerically, in which the compressive forces are not aligned with the underlying geometry.